

7-1-2003

Infrared spectroscopic ellipsometry study of vinylidene fluoride (70%)-trifluoroethylene (30%) copolymer Langmuir-Blodgett films

Mengjun Bai

University of Nebraska-Lincoln, baime@missouri.edu

Matt Poulsen

University of Nebraska-Lincoln, map@suiter.com

A.V. Sorokin

University of Nebraska - Lincoln

Stephen Ducharme

University of Nebraska, sducharme1@unl.edu

C.M. Herzinger

J. A. Woollam Company, Lincoln, Nebraska

See next page for additional authors

Follow this and additional works at: <http://digitalcommons.unl.edu/physicsducharme>



Part of the [Physics Commons](#)

Bai, Mengjun; Poulsen, Matt; Sorokin, A.V.; Ducharme, Stephen; Herzinger, C.M.; and Fridkin, V.M., "Infrared spectroscopic ellipsometry study of vinylidene fluoride (70%)-trifluoroethylene (30%) copolymer Langmuir-Blodgett films" (2003). *Stephen Ducharme Publications*. 8.

<http://digitalcommons.unl.edu/physicsducharme/8>

This Article is brought to you for free and open access by the Research Papers in Physics and Astronomy at DigitalCommons@University of Nebraska - Lincoln. It has been accepted for inclusion in Stephen Ducharme Publications by an authorized administrator of DigitalCommons@University of Nebraska - Lincoln.

Authors

Mengjun Bai, Matt Poulsen, A.V. Sorokin, Stephen Ducharme, C.M. Herzinger, and V.M. Fridkin

Infrared spectroscopic ellipsometry study of vinylidene fluoride (70%)-trifluoroethylene (30%) copolymer Langmuir–Blodgett films

Mengjun Bai, Matt Poulsen, A. V. Sorokin,^{a)} and Stephen Ducharme^{b)}

Department of Physics and Astronomy, Center for Materials Research and Analysis, University of Nebraska, Lincoln, Nebraska 68588-0111

C. M. Herzinger

J. A. Woollam Company, 645 M St., Lincoln, Nebraska 68508

V. M. Fridkin

Institute of Crystallography, Russian Academy of Sciences, Moscow 117333, Russia

(Received 10 March 2003; accepted 8 April 2003)

We report the studies of the molecular conformation and chain orientations through characterization of the vibrational modes in crystalline Langmuir–Blodgett films of the polyvinylidene fluoride/trifluoroethylene copolymer. The infrared spectra obtained by polarized reflectometry and ellipsometry showed that the ferroelectric phase has predominantly all-trans conformation and the paraelectric phase has predominantly alternating trans-gauche conformation, as in solvent-formed films of the same copolymer. The results showed that the polymer chains are predominantly parallel to the film plane with a random in-plane orientation and most of the ferroelectric phase vibrational mode behaviors are consistent with the published mode assignments. The ferroelectric phase optical dispersion curves in the infrared range were extracted from the data analysis based on a uniaxial model. © 2003 American Institute of Physics. [DOI: 10.1063/1.1578697]

I. INTRODUCTION

Polyvinylidene fluoride (PVDF) and its copolymers with trifluoroethylene (TrFE) and tetrafluoroethylene (TeFE) have been studied for many years since the discovery of piezoelectricity (1969)¹ and pyroelectricity (1971)² in PVDF and confirmation of ferroelectricity (1980) in the PVDF/TrFE copolymers.³ For PVDF, molecular modeling and experimental studies have identified several basic structures and conformations.^{4–7} The main intrachain vibrational modes range in frequency from about 400 to about 3000 cm^{-1} , while the interchain crystal vibrational modes are below 100 cm^{-1} .⁸ The frequencies of many intrachain vibrational modes of PVDF have been determined from molecular modeling by several groups^{4,5} and are summarized by Tashiro.⁸ One difficulty with matching experimental and calculated spectra is the polymorphous nature of the samples. Samples prepared by the spin-coated, solution-cast, and vacuum-evaporated methods and treated with different procedures generally contained lamellar structures could have slightly different physical properties. The PVDF/TrFE copolymers have essentially the similar structure and conformation as PVDF.^{8,9} Recently, high-quality Langmuir–Blodgett (LB) films of the PVDF/TrFE copolymer have been made by our group.^{10–12} X-ray diffraction studies¹³ showed that the films in ferroelectric phase (β phase) with all-trans conformation have (110) orientation. Scanning tunneling microscopy,¹²

scanning electron microscopy,¹⁴ and atomic force microscopy results revealed no lamellar structures in the copolymer LB films.

Vibrational spectroscopy is a powerful tool for determining molecular structure. The frequencies and intensities of infrared (IR) modes can be correlated to molecular conformation and structure while the optical polarization of the modes reveals molecular orientation from the direction of the transition dipole. The molecular modeling calculations on the all-trans conformation of PVDF identify seven strong infrared-active modes in the range 600–1600 cm^{-1} . Some of the modes, the ones locating in a single monomer, are generally insensitive to chain conformation, but they are useful for determining chain orientation. For example, the CH_2 and CF_2 wagging modes have the transition dipole moments parallel to the chain axis. Modes involving two or more monomers are very sensitive to the conformation. For example, the 1290 cm^{-1} mode is found only in the ferroelectric all-trans conformation.¹⁵ When polarized light is incident on the film surface, the intensity of the reflected light is determined by the complex effective Fresnel coefficients $r_s(\nu, \theta)$ and $r_p(\nu, \theta)$, where the subscripts “s” and “p” refer to the polarization component parallel and perpendicular to the plane of incidence, respectively. In polarized reflectance spectroscopy, the ratio of reflected to incident intensities is measured with both s- and p-polarization, as a function of frequency ν and angle of incidence θ (measured from the surface normal), yielding the reflectance $R_{ss}(\nu, \theta) = |r_s(\nu, \theta)|^2$ and $R_{pp}(\nu, \theta) = |r_p(\nu, \theta)|^2$. In spectroscopic ellipsometry,¹⁶ both the incident and reflected polarization states are measured, yielding the complex ratio $\rho(\nu, \theta) = \tan \psi(\nu, \theta) \exp i\Delta(\nu, \theta) = r_s(\nu, \theta)/r_p(\nu, \theta)$, where $\tan \psi(\nu, \theta)$ is the reflectance ratio

^{a)}Also with the Department of Physics, Ivanovo State University, Ivanovo 153025, Russia.

^{b)}Electronic mail: sducharme1@unl.edu

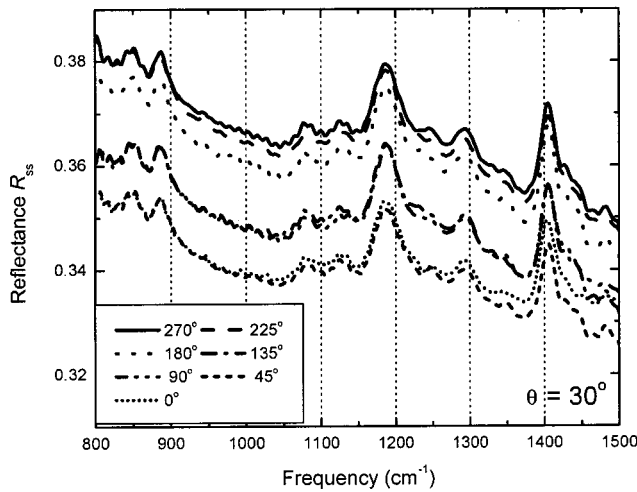


FIG. 1. The IR spectra of the reflectance R_{ss} as a function of azimuthal rotation angle from a 115-ML sample deposited on Si (100) and annealed at 120 °C for one hour. The incident angle was fixed at $\theta=30^\circ$.

and $\Delta(\nu, \theta)$ is the retardance. The measurable quantities $R_{ss}(\nu, \theta)$ and $R_{pp}(\nu, \theta)$, $\psi(\nu, \theta)$, and $\Delta(\nu, \theta)$ are related to the film optical properties and thickness. In this work we report the studies of the LB films made from the PVDF/TrFE copolymer using polarized spectroscopic ellipsometry.

II. EXPERIMENT

The films were made by the horizontal (Schaefer) variation of the Langmuir–Blodgett technique using a NIMA model 622C automated LB trough filled with ultra-pure ($>18 \text{ M}\Omega \text{ cm}$) water. Substrates used in this work were electronic-grade Si (100) or (111) wafers. The copolymer of polyvinylidene fluoride/trifluoroethylene (70/30 molar ratio) was dissolved in dimethyl sulfoxide at 80 °C to form a 0.1% solution (by weight). Approximately 5 mL of the solution at room temperature was dispersed on the surface of the water, which was kept at 20 °C. The surface film was compressed slowly to a surface pressure of 5 mN/m to form a uniform monomolecular layer (ML) or Langmuir film, and the pressure was kept constant during film transfer. Films of different thickness were prepared by repeated transfer.¹⁷ The films were prepared on doped Si wafers (with native oxide layer), because they are opaque to infrared in the measurement range, so we do not need to account for the reflection from the back of the substrate. All the samples were annealed at either 120 or 130 °C for one hour followed by cooling at a rate of 1 °C/min to room temperature.

The infrared spectra of the ellipsometric parameters $\psi(\nu, \theta)$ and $\Delta(\nu, \theta)$ and the polarized reflectances $R_{ss}(\nu, \theta)$ and $R_{pp}(\nu, \theta)$ were obtained at multiple incident angles with an Infrared Variable Angle Spectroscopic Ellipsometry system (IR-VASE®). The system consists of a Fourier-transform infrared spectrometer coupled with a rotating-analyzer variable-angle ellipsometer and is capable of precise determination of the optical constants of thin films over the frequency range 200–7000 cm^{-1} with a resolution of 2 cm^{-1} or better.

III. RESULTS AND DISCUSSION

A. Conformation and vibrational mode orientation

The absorption intensity of the vibrational modes depends on the matrix elements $\mathbf{I} \sim \Sigma [\boldsymbol{\mu}_j(\nu) \cdot \mathbf{E}_i]^2$, so it is sensitive to the angle between the electric field \mathbf{E}_i of the light and the transition dipole $\boldsymbol{\mu}_j(\nu)$. Light polarization state dependence of the absorption coefficients can be used to determine the orientation of the transition dipoles. The IR spectra of the reflectance were recorded from a 115-ML LB film annealed at 120 °C. The cross-sectional area of the beam was about 100 mm^2 . Figure 1 shows the reflectance spectra R_{ss} as a function of azimuthal rotation angle about the film normal, with a fixed incident angle $\theta=30^\circ$ (The overall reflectance fluctuated by about $\pm 5\%$ due to alignment drift as the sample was rotated.). As the angle of incidence θ increased, the in-plane reflectance R_{ss} increased and the out-of-plane reflectance R_{pp} decreased according to the Fresnel law of reflectance. Figure 2 shows the normalized reflectance R_{ss} and R_{pp} . The raw data of the reflectance R_{ss} and R_{pp} are divided by the reflectance values at 1000 cm^{-1} , where no vibrational mode is registered. Table I lists the R_{ss} and R_{pp} values at 1000 cm^{-1} before normalization. Figure 3 shows the spectra R_{pp} at low-incident angle ($\theta=30^\circ$) and high-incident angle ($\theta=70^\circ$) separately for clarity. The spectra shown in Figs. 1–3 are similar to the β phase spectra obtained from the copolymer solution-cast films¹⁸ and vacuum-evaporated films.¹⁵ Seven main peaks are evident at 1428, 1403, 1290, 1182, 1070, 886, and 850 cm^{-1} .

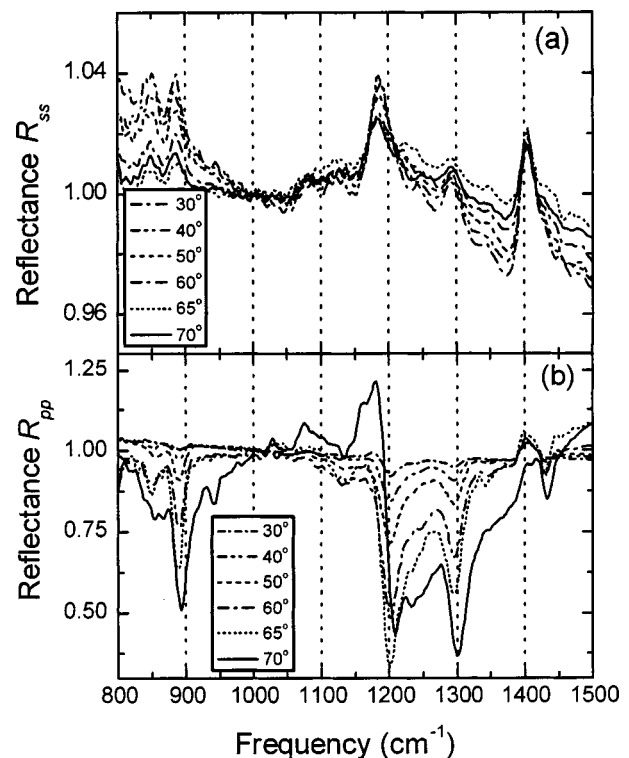


FIG. 2. IR spectra of the reflectance (a) R_{ss} and (b) R_{pp} at several angles of incidence θ for s - and p -polarized incident light recorded from the same 115-ML sample used for Fig. 1. The spectra are all normalized to the reflectance at 1000 cm^{-1} .

TABLE I. The experimental values of R_{ss} and R_{pp} at 1000 cm^{-1} before normalizing at several incident angles, obeying the Fresnel law of reflectance.

Incident angle	30°	40°	50°	60°	65°	70°
R_{ss}	0.3737	0.4081	0.4631	0.4989	0.5185	0.5229
R_{pp}	0.2562	0.2056	0.1449	0.0725	0.0383	0.0171

From Figs. 1–3, we can obtain useful information about the orientation of the transition dipole moments. The in-plane reflectance R_{ss} spectra did not change significantly with the azimuthal angle, as shown in Fig. 1, or with the incident angle, as shown in Fig. 2(a). From these observations, we can conclude that the film is optically isotropic in the film plane, indicating that the crystals have random in-plane orientation. From the reflectance spectra R_{pp} shown in Fig. 2(b), we can see that the intensities of the peaks at 850, 886, 1290, and 1428 cm^{-1} increase with the increasing incident angles (up to 70°), indicating that the transition dipoles of these modes have predominantly out-of-plane orientation. The intensity of the peak at 1182 cm^{-1} does not increase as fast as the one at 1290 cm^{-1} , indicating that the transition dipoles of this mode also have some out-of-plane orientation but are not completely normal to the film. Also from Figs. 2(b) and 3, we can see that the in-plane intensity of the peak at 1403 cm^{-1} is greater than the out-of-plane intensity and decreases in intensity with the increasing incident angle, indicating that the transition dipole of this mode is predominantly in the film plane. According to Tashiro⁸ and Tashiro, Takano, and Kobayashi¹⁸ this mode combines the CC out-of-phase symmetrical stretching and CH_2 wagging motions,

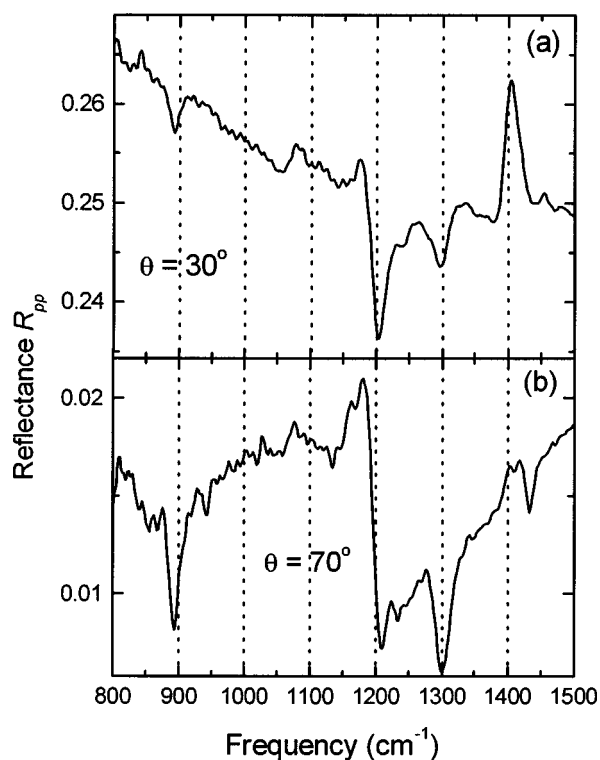


FIG. 3. The low-angle ($\theta=30^\circ$) and high-angle ($\theta=70^\circ$) reflectance for p -polarization R_{pp} from the 115-ML sample.

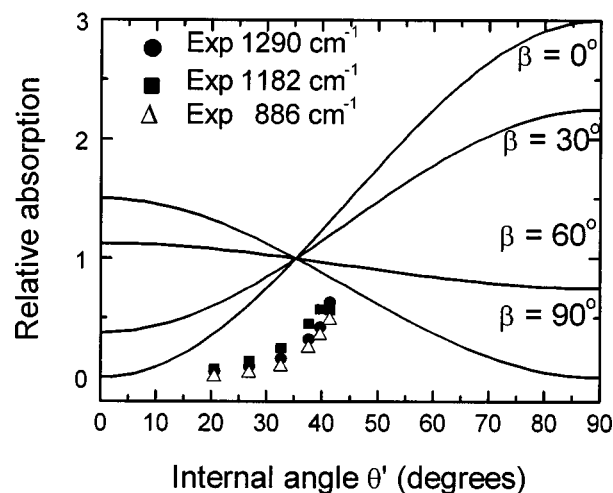


FIG. 4. Dependence of the intensities of three peaks of the p -polarized reflectance R_{pp} vs internal angle for the 115-ML film, from the data shown in Fig. 2. The solid lines show the expected dependence of the absorption coefficient for transition dipoles tilted by angles $\theta=0^\circ$, 30° , 60° , and 90° from the film normal.

which are along the chain direction (B_1) for the β phase all-trans conformation, so we can conclude that the polymer chains of the LB films are mostly parallel to the film plane, with a random in-plane orientation.

The polarization anisotropy of the vibrational modes is calculated as follows. We assume the film is isotropic about an axis perpendicular to the film. The reflectance R_{pp} of a mode $\mu_j(\nu)$ is obtained by averaging about the azimuthal angle. Figure 4 shows the azimuthally averaged reflectance versus internal (refracted) angle θ' for the transition dipoles oriented at 0° , 30° , 60° , and 90° from the film normal and the experimental reflectance R_{pp} of the three peaks at 1290, 1182, and 886 cm^{-1} from Fig. 2(b). The internal angles are obtained by assuming the averaged refractive index is 1.42 for the entire spectral range. From the optical constants obtained by analyzing the VASE data in the following section, we find this is a very good approximation. From Fig. 4, we conclude that the transition dipole moments of these three modes are predominantly out-of-plane, and therefore have more A_1 character than B_2 character. The experimental curves showed an increasing trend with larger incident angles, while the theoretical prediction showed a similar trend for the angles 0° and 30° , even though the experimental data are the combination of the optical absorption and dispersion as well as the substrate contribution. But with the present data, we cannot quantitatively distinguish the modes with its orientation normal to the film (0°) or 30° from the normal. The other two out-of-plane modes at 850 and 1428 cm^{-1} also showed the increasing trend with increasing incident angle.

From the above analysis of the reflectance data and the mode symmetries, we find good correspondence for the peak positions and some of the mode orientations between the stronger IR peaks and the published mode assignments,^{4,8} as summarized in Table II. However, two peaks at 886 and 1182 cm^{-1} did not follow the B_2 mode behaviors as expected. Because the relative intensity of the peak at 886 cm^{-1} in-

TABLE II. List of some dominant vibrational modes in the ferroelectric phase, including the measured frequencies, sensitivity to the conformation, transition dipole orientation (TDO) relative to the chain, the calculated frequencies, and mode assignments.

Observed mode frequency ^a (cm ⁻¹)	Sensitivity to conformation ^a	TDO relative to film plane ^a	Dominant mode character ^a (cm ⁻¹)	Observed mode frequency ^b (cm ⁻¹)	Calculated mode frequency ^c (cm ⁻¹)	Calculated mode frequency ^d (cm ⁻¹)
1428	Very weak	⊥	A ₁	1428(A ₁)	1434(A ₁)	1426(A ₁)
1403	Strong	∥	B ₁ or B ₂	1398(B ₁)	1408(B ₁)	1399(B ₁)
1290	Strong	⊥	A ₁	1273(A ₁)	1283(A ₁)	1273(A ₁)
1182	Medium	⊥	A ₁	1177(B ₂)	1177(B ₂)	1164(B ₂)
886	Medium	⊥	A ₁	880(B ₂)	883(B ₂)	882(A ₁)
850	Strong	⊥	A ₁	840(A ₁)	844(A ₁)	843(B ₂)

^aThis work, using LB films of the 70:30 copolymer.

^bFrom Tashiro⁸ using spun films of the 70:30 copolymer.

^cFrom Tashiro⁸ molecular modeling of PVDF.

^dFrom Karasawa and Goddard⁴ molecular modeling of PVDF.

increases monotonically with incident angle (see Figs. 2 and 3) like the one at 1290 cm⁻¹, and the relative intensity of the peak at 1182 cm⁻¹ also increased with increasing incident angle but it decreased at external incident angle 70°. It is possible that these two peaks are both involved in two or more vibrational modes, one part is associated with a single monomer molecular conformation and the others to two or more monomers. On the other hand, comparing to the IR spectra in the ferroelectric and paraelectric phases shown in Fig. 5, we can see that the peaks at 850 and 1290 cm⁻¹ are much stronger in the ferroelectric phase than in the paraelectric phase, so they probably involve cooperative motion of two or more monomers. Some of the peaks are sensitive to the conformation, such as the peaks at 886 and 1182 cm⁻¹, because their intensities changed between phases, and may involve both single and multiple monomer modes. Other peaks are not sensitive to the conformation (they correspond to modes located in a single monomer), such as the one at 1428 cm⁻¹, and so do not change between phases. The CH₂ wagging mode at 1403 cm⁻¹ (Fig. 5) in the ferroelectric phase softens to 1396 cm⁻¹ with the reduced backbone stiff-

ness of the trans-gauche (TG) conformation in the paraelectric phase, and the ellipsometric phase of this mode reverses from down (in the paraelectric phase) to up (in the ferroelectric phase) because of the larger corresponding change in the refractive index. In the paraelectric phase, the broadening of the peak at the 1250 cm⁻¹ is possibly due to the overlap of several modes in this range.^{4,8} Similar IR spectral changes induced by the conformation change were also observed in the solvent-formed copolymer films.¹⁵

Earlier molecular modeling by Kobayashi, Tashiro, and Tadokoro (1975)¹⁹ initially assigned the mode at 886 cm⁻¹ to be as A₁ and the mode at 1182 cm⁻¹ to be as B₂ and later assigned both to B₂ characters.²⁰ The calculations from Karasawa & Goddard in 1992⁴ gave the modes A₁ and B₂ characters, respectively. As mentioned earlier, the PVDF/TrFE copolymers have similar structure and conformation as PVDF. Experimental studies on the PVDF/TrFE (73/27) copolymer by Tashiro and Kobayashi in 1994¹⁵ showed that poling the film increased the normal component of the 850, 1290, and 1428 cm⁻¹ modes, showing A₁ character, and decreased the normal component of the 886 and 1182 cm⁻¹ modes, showing B₂ character for these two modes.^{15,18} There are several reasons that the poling data might have been misleading. First, recall that these two peaks could come from three crystalline phases as well as amorphous material in the solvent-formed films.^{8,15} Since both peaks decrease in intensity in the paraelectric phase (Fig. 5), they must involve multiple monomers and are therefore sensitive to the proportion and orientation of the β phase. Second, poling the films should orient all CF₂ dipoles toward the film normal. For highly crystalline films, contributions from the boundaries and noncrystalline region are not significant. But, this contribution could not be neglected, even after poling, for the films with lower crystallinity (The copolymer films made by different methods could have crystalline domains embedded in an amorphous matrix with the dominant phase and the crystallinity depending on the preparation procedures and the processing methods.^{8,9}). More specifically, for the copolymer films in the ferroelectric β phase, poling the films may enlarge the domain sizes slightly by reducing the number of TG bond sequences. So if the peaks do not correspond to a single

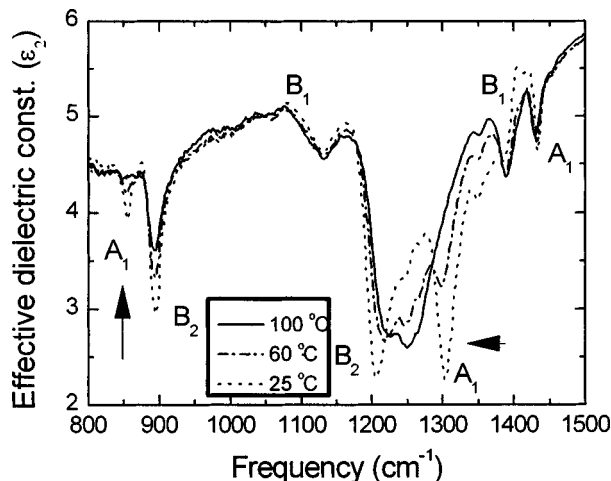


FIG. 5. IR-VASE spectra at incident angle $\theta=55^\circ$ recorded from a 50-ML sample at 100 °C (paraelectric phase), 60 °C, and 25 °C (ferroelectric phase). The sample was heated to 120 °C for 30 min to ensure it was entirely in the paraelectric phase then cooled down slowly at the rate of 1 °C/min.

mode, the intensity change due to poling is more complicated, depending on the predominant mode contribution to the intensity, and so it is sensitive to the film treatment procedures and crystallinity. If a peak is a mixture of the A_1 mode and a mode from the predominant TG sequences, the intensity may decrease after poling due to the reduction in the number of the TG sequences. If a peak is a mixture of B_2 and a mode from the TG sequences, there will be similar spectral changes. Comparing to the polarized IR reflectance from the copolymer LB films without poling ($\theta=70^\circ$, see Fig. 3) and the data from solution-cast films ($\theta=84^\circ$) after poling,^{8,15} and the similarity of the spectra and the stronger intensity of the peak at 1290 cm^{-1} for the LB films, we may conclude that the CF_2 dipoles are more highly aligned in the LB films. The observed inconsistency in the normalized reflected intensity of the peaks at 886 and 1182 cm^{-1} in the LB films can be explained reasonably by the mixed-modes assumption.

Previous results obtained by the x-ray^{13,21} and neutron²² diffraction studies of the LB films in the β phase showed a sharp peak corresponding to the d -spacing 4.5 \AA , similar to the solvent-formed films,^{8,9} indicating that the β phase (110) crystal orientation was predominant in the LB films, which would put the static dipole polarization at about $\pm 30^\circ$ from the normal according to the standard C_{2v} crystal symmetry. However, photoemission²³ electron energy studies imply that the dipoles are mostly out of the film plane. Whether this inconsistency is due to mosaic randomization in the LB films or incorrect crystal structure assignment is not clear. Meanwhile, the complex sample structure containing Si substrate, Si oxide, and the copolymer LB films effectively prevents a quantitative determination of the optical properties from the polarized reflectance data. For that, we turn to spectroscopic ellipsometry.

B. Variable angle spectroscopic ellipsometry (VASE) data analysis

In order to extract the optical properties of the film, the VASE data can be analyzed by using a parametric model that is adjusted to fit the measurement data.²⁴ The crystalline copolymer is fundamentally biaxial, and anisotropic films of high crystallinity with in-plane orientation of the polymer chains have been made by the thermal-mechanical processing methods.^{25,26} The LB films may also consist of a polycrystalline mosaic that renders the optical properties isotropic within the film plane. Previous studies of the LB copolymer films^{11–13,21,22,27} showed that the surface layer frequently has parallel chain alignment over regions on the scale of 1 mm^2 . The polarized light reflectance studies described in the previous section show that the chains are parallel to the film surface with the CF_2 dipoles oriented nearly normal for the thicker samples, but did not reveal significant in-plane anisotropy, consistent with a crystalline mosaic. So a uniaxial model is used to represent both in-plane and out-of-plane optical properties for the VASE data analysis. The model consists of several Lorentz oscillators with the form $\varepsilon(v) = \varepsilon_1(v) + i\varepsilon_2(v) = \sum A_k / (v_k^2 - v^2 - iB_kv) = \{n(v) + ik(v)\}^2$, where $\varepsilon_1(v)$ and $\varepsilon_2(v)$ are the real part and

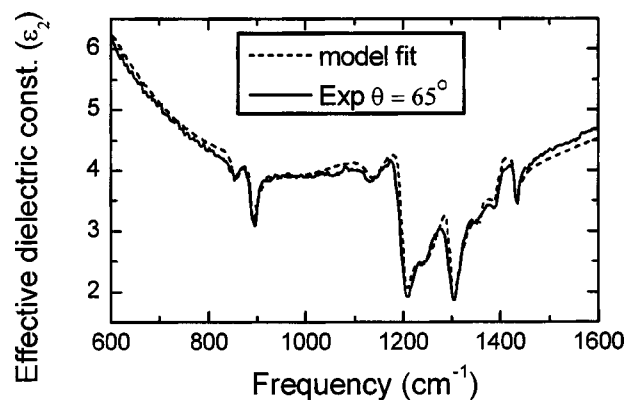


FIG. 6. IR-VASE data at the angle of incidence $\theta=65^\circ$ recorded from a 100-ML sample and the Lorentz model fit in the range $600\text{--}1600\text{ cm}^{-1}$.

imaginary part of the dielectric constant tensors, $n(v)$ and $k(v)$ are the refractive index and attenuation constant tensors, A_k is the amplitude of the absorption oscillator, v_k is the absorption oscillator frequency center, B_k is the absorption oscillator band width, and v is the absorption oscillator frequency.

The VASE data were fit with a regression technique to determine the optical constants, absorption coefficients, and the film thickness. This is done by minimizing the mean square error function for a set of Lorentz oscillators and assuming uniaxial symmetry.²⁸ For a single sample, even data acquisition at multiple incident angles is insufficient to uniquely determine the optical constants and thickness of an optically thin film because of correlations among fitting parameters.¹⁶ But if we have several samples with different thicknesses, and assume their optical constants are independent of the thickness, a powerful multisample data analysis technique can be used to get the results more accurately by greatly reducing the correlation among the fitting parameters.²⁸

The IR-VASE spectra of all four films of PVDF/TrFE (70/30) copolymer of nominal thickness 55, 65, 80, and 100 ML and annealed at 120°C and a reference substrate from the same batch were recorded in the ranges $200\text{--}7000\text{ cm}^{-1}$. The optical properties of the substrate are also very important, so they are independently characterized by the ellipsometry before the LB film deposition. The four spectra were simultaneously fit using multisample analysis to a multilayer uniaxial model with following features. The model consists of doped Si substrate, silicon oxide layer, and uniaxial polymer film with 16 oscillators, 8 with dipole moment perpendicular to the film and 8 parallel. Figure 6 shows the data and the model fit for one representative spectra, for the 100 ML film at an angle of incidence $\theta=65^\circ$. The fits for the other spectra were similarly accurate. The dispersion at low wave number (see Fig. 6) was entirely due to the substrate. Figure 7 shows both in-plane and out-of-plane components of the refractive indices n_{\parallel} and n_{\perp} and the attenuation constants k_{\parallel} and k_{\perp} . Most of the absorption peaks show up in both k_{\parallel} and k_{\perp} with similar positions and shapes but different magnitudes. The exception is the mode at 1403 cm^{-1} , which corresponds to the in-chain CC out-of-phase

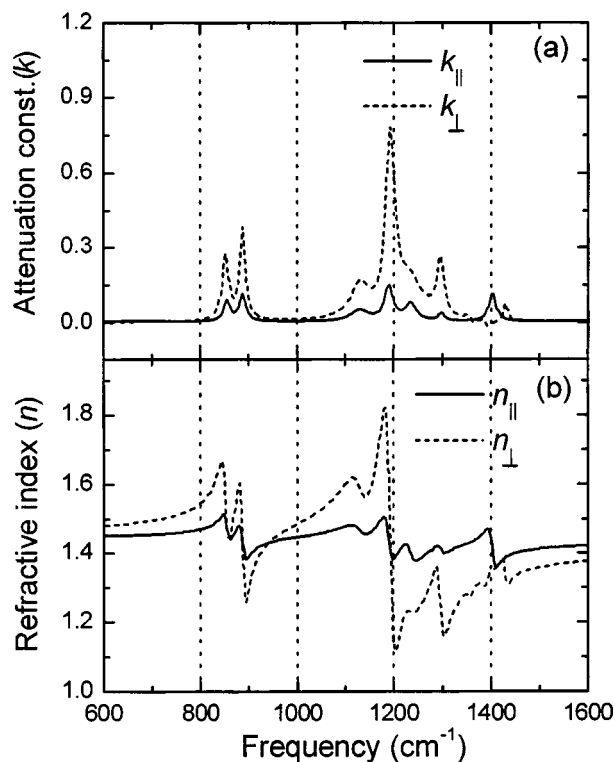


FIG. 7. The in-plane (\parallel) and out-of-plane (\perp) optical properties of the LB films obtained from the IR-VASE data analysis. (a) The attenuation constants k_{\parallel} and k_{\perp} and (b) the refractive indices n_{\parallel} and n_{\perp} .

symmetrical stretching and CH₂ wagging mode and therefore is much stronger in k_{\parallel} .

The results are consistent with the polarized reflectance measurements, which showed that the chains lay predominantly in the film plane with a random azimuthal distribution while the A_1 and B_2 modes are active both in-plane and out-of-plane (Figs. 1–3). Other unidentified modes may overlap some of the all-trans β phase modes as mentioned above and also contribute to the attenuation constants and the optical refractive indices. The weaker change of the in-plane refractive index n_{\parallel} and the stronger change of the out-of-plane refractive index n_{\perp} are also consistent with the random in-plane distribution of the transition dipoles.

IV. CONCLUSIONS

The vibrational mode frequencies and orientations in the ferroelectric phase of the PVDF/TrFE copolymer LB films were determined by a combination of polarized reflectance spectroscopy and spectroscopic ellipsometry. The results showed that the polymer chains are predominantly parallel to the film plane with random in-plane orientation. The results also confirmed that the all-trans conformation was predominant in the ferroelectric phase and trans-gauche conformation was predominant in the paraelectric phases. The ferroelectric phase optical dispersion in the infrared range was extracted from the data analysis based on a uniaxial model.

ACKNOWLEDGMENTS

We thank Daniel W. Thompson from the Department of Electrical Engineering, University of Nebraska for his kind assistance with the VASE systems. This work was supported by the National Science Foundation Small-Business Innovation Research Program (DMI-9901510), the Office of Naval Research, and the Nebraska Research Initiative.

- ¹H. Kawai, Jpn. J. Appl. Phys. **8**, 975 (1969).
- ²J. G. Bergman, J. H. McFee, and G. R. Crane, Appl. Phys. Lett. **18**, 203 (1971).
- ³T. Furukawa, M. Date, E. Fukada, Y. Tajistu, and A. Chiba, Jpn. J. Appl. Phys., Part 2 **19**, L109 (1980).
- ⁴N. Karasawa and W. A. Goddard III, Macromolecules **25**, 7268 (1992).
- ⁵K. Tashiro, Y. Abe, and M. Kobayashi, Ferroelectrics **171**, 281 (1995).
- ⁶E. Bellet-Amalric and J. F. Legrand, Eur. Phys. J. B **3**, 225 (1998).
- ⁷A. J. Lovinger, in *Developments in Crystalline Polymers-I*, edited by D. C. Bassett (Applied Sciences, London, 1982), p. 195.
- ⁸K. Tashiro, in *Ferroelectric Polymers*, edited by H. S. Nalwa (Marcel Dekker, New York, 1995), p. 63.
- ⁹T. Furukawa, Phase Transitions **18**, 143 (1989).
- ¹⁰A. Bune, S. Ducharme, V. M. Fridkin, L. Blinov, S. Palto, N. Petukhova, and S. Yudin, Appl. Phys. Lett. **67**, 3975 (1995).
- ¹¹S. Ducharme, S. P. Palto, and V. M. Fridkin, in *Handbook of Thin Film Materials*, Vol. 3, edited by H. S. Nalwa (Academic, New York) p. 545.
- ¹²A. V. Bune, V. M. Fridkin, S. Ducharme, L. M. Blinov, S. P. Palto, A. V. Sorokin, S. G. Yudin, and A. Zlatkin, Nature (London) **391**, 874 (1998).
- ¹³J. Choi, C. N. Borca, P. A. Dowben, A. Bune, M. Poulsen, S. Pebley, S. Adenwalla, S. Ducharme, L. Robertson, V. M. Fridkin, S. P. Palto, N. N. Petukhova, and S. G. Yudin, Phys. Rev. B **61**, 5760 (2000).
- ¹⁴M. Bai, M. Poulsen, A. V. Sorokin, S. Ducharme, and V. M. Fridkin, Mater. Res. Soc. Symp. Proc. **698**, EE2.8.1 (2002).
- ¹⁵K. Tashiro and M. Kobayashi, Spectrochim. Acta, Part A **50A**, 1573 (1994).
- ¹⁶R. M. A. Azzam and N. M. Bashara, *Ellipsometry and Polarized Light* (North Holland, Amsterdam, 1977), 529 pages.
- ¹⁷A. Sorokin, S. Palto, L. Blinov, V. Fridkin, and S. Yudin, Mol. Mater. **6**, 61 (1996).
- ¹⁸K. Tashiro, K. Takano, and M. Kobayashi, Ferroelectrics **57**, 297 (1984).
- ¹⁹M. Kobayashi, K. Tashiro, and H. Tadokoro, Macromolecules **8**, 158 (1975).
- ²⁰K. Tashiro, Y. Itoh, M. Kobayashi, and H. Tadokoro, Macromolecules **18**, 2600 (1985).
- ²¹M. Poulsen, S. Adenwalla, S. Ducharme, V. M. Fridkin, S. P. Palto, N. N. Petukhova, and S. G. Yudin, in *Proceedings of the Ferroelectric Thin Films IX*, Nov. 27–Dec. 1, edited by P. C. McIntyre, S. R. Gilbert, Y. Miyasaka, R. W. Schwartz, and D. Wouters, Vol. 655 (Materials Research Society, Boston, 2001), p. CC10.14.1.
- ²²C. N. Borca, S. Adenwalla, J. Choi, P. T. Sprunger, S. Ducharme, L. Robertson, S. P. Palto, J. Liu, M. Poulsen, V. M. Fridkin, H. You, and P. A. Dowben, Phys. Rev. Lett. **83**, 4562 (1999).
- ²³J. Choi, S.-J. Tang, P. T. Sprunger, P. A. Dowben, J. Braun, E. W. Plummer, V. M. Fridkin, A. V. Sorokin, S. P. Palto, N. Petukhova, and S. G. Yudin, J. Phys.: Condens. Matter **12**, 4735 (2000).
- ²⁴C. M. Herzinger, P. G. Snyder, B. Johs, and J. A. Woollam, J. Appl. Phys. **77**, 1715 (1995).
- ²⁵K. Omote, H. Ohigashi, and K. Koga, J. Appl. Phys. **81**, 2760 (1997).
- ²⁶J. K. Krüger, B. Heydt, C. Fischer, J. Baller, R. Jiménez, K.-P. Bohn, B. Servet, P. Galtier, M. Pavel, B. Ploss, M. Beghi, and C. Bottani, Phys. Rev. B **55**, 3497 (1997).
- ²⁷S. Palto, L. Blinov, E. Dubovik, V. Fridkin, N. Petukhova, A. Sorokin, K. Verkhovskaya, S. Yudin, and A. Zlatkin, Europhys. Lett. **34**, 465 (1996).
- ²⁸C. M. Herzinger, H. Yao, P. G. Snyder, F. G. Celii, Y. C. Kao, B. Johs, and J. A. Woollam, J. Appl. Phys. **77**, 4677 (1995).